INTERNATIONAL JOURNAL OF MECHANICS
DOI: 10.46300/9104.2023.17.12 Volume 17, 2023

Cracks Classification using Acoustic Emission Technique on a Reinforced Concrete Beam

Antonella Bianca Francavilla
University of Salerno, Department of Civil Engineering
Via Giovanni Paolo II, 132 - 84084
Fisciano (SA), Italy

Paola Barra
University of Salerno, Department of Civil Engineering
Via Giovanni Paolo II, 132 - 84084
Fisciano (SA), Italy

Domenico Rossi
University of Salerno, Department of Civil Engineering
Via Giovanni Paolo II, 132 - 84084
Fisciano (SA), Italy

Massimo Latour
University of Salerno, Department of Civil Engineering
Via Giovanni Paolo II, 132 - 84084
Fisciano (SA), Italy

Claudio Guarnaccia
University of Salerno, Department of Civil Engineering
Via Giovanni Paolo II, 132 - 84084
Fisciano (SA), Italy

Gianvittorio Rizzano
University of Salerno, Department of Civil Engineering
Via Giovanni Paolo II, 132 - 84084
Fisciano (SA), Italy

Received: March 29, 2023. Revised: June 21, 2023. Accepted: August 18, 2023. Published: September 12, 2023.

***Abstract*— The usage of non-destructive techniques for structure's state assessment is highly desirable because they offer the possibility to monitor continuously and in a non-invasive manner the sign of failures of any structure. Among the several techniques proposed over the years, Acoustic Emission (AE) seems very promising. Such a technique, which applies to various materials, consents to the evaluation of micro-fractures generated during failure by detecting their acoustic emission through sensors located on the surface of the material itself. Concrete beam failure is suitable for such kind of procedure. It has been widely investigated through AE, but despite the many literature contributes, there still is a scarcity of practical applications on real structures, and no consensus on protocols. In this work, an AE technique has been paired with a four-point bending test to try and find a robust and reliable experimental setup for AE application on concrete beams. Results show a proper classification of the occurring cracks, which change according to different zones of the concrete beam and different load values. Axial crack signals exhibit different features concerning shear crack ones. In such a way, the categorization of damages can be performed and crosschecked with the theoretical expectations. All these results suggest that the proposed setup can be used as a possible protocol for practical AE measurements.**

Keywords* — *Acoustic Emissions-AE, experimental AE analysis, Non-Destructive Technique, Reinforce concrete beam, cracks classification.

I. Introduction

The durability of structures poses a critical concern that every construction professional must confront. Each structure is subject to deterioration due to operating loads, fatigue, and chemical reactions to environmental agents. The assessment of a construction state is, then, of great importance for the safety of people living or working in it, [1]. Structure's state assessment, anyway, cannot be (always) carried out through invasive techniques due to the high costs and the connected risks. Nonetheless, constant and non-invasive monitoring over time would be highly desirable to assure a prompt detection of minimal signs of failure, thus permitting a fast intervention when needed and avoiding demanding costs, [2].

Several approaches have been proposed to reach such a goal, and they are generally referred to as Non-Destructive testing Techniques (NDT), [3]. Among them, Acoustic Emission (AE) is one of the most promising ones since it can provide a lot of details about the state of the material by detecting, through piezoelectric sensors on the surface of a structure, the onset of micro-cracks by catching the elastic waves propagating from them, [4]. Such a technique is advantageous since it allows for identifying the deterioration process of a structure already at a microscopic level when structural damages can be faced with early intervention and localized maintenance, [5].

Many studies are reported in literature where the AE technique is applied to structural monitoring in several fields. As examples, in [6], the authors investigated, through AE, the generation of micro-fractures in notched concrete beams under three-point bending. In [7], [8], the AE technique has been used not only to assess micro-fractures generation (under four-point bending) but also the correlation of the damage with the AE parameters. These and other works clearly state that AE is a powerful technique for assessing microfractures, even in the very early stages of their generation, and candidate such technique to be a powerful one for a continued and non-invasive assessment of the deterioration of a structure. The possibility to predict forthcoming cracks in the specimen, earlier than detection by visual inspection, also makes such a technique worthy of in-depth study and analysis. In [9], [10], authors used AE to assess bridge stability and deterioration. In [11], AE has been used for the analysis of carbon-fiber-reinforced polymer (CFRP), while in [12], authors analyzed the stability of a gas metal arc welding process. These examples show how AE usage is widespread and adjustable to a plethora of structural situations. Our groups also contributed over time, like in [13], [14], where the generation of micro-fractures on a concrete beam undergoing four points bending test was analyzed with AE.

Relating to the evaluation of concrete beams, despite all the complex works in literature, there is a scarcity of practical applications on real structures, and there is no consensus on the technique specification or protocols to follow, mainly because they are primarily referring to laboratory tests. In this study, an AE technique was utilized in conjunction with four-point bending tests performed on a Reinforced Concrete (RC) beam at the StrEngTH laboratory of the Department of Civil Engineering, University of

This work has been supported by "Consorzio della Rete dei Laboratori Universitari di Ingegneria Sismica e Strutturale" (ReLUIS) under the project "ReLUIS-Ponti", Sub-task 3.2.1.

Salerno. The aim was to assess the identification of cracks through acoustic emission during a bending test, to classify their typology (axial or shear stress cracks), and to localize them, thus identifying the region of the beam where the damages more frequently occur. The combination of localization and classification provides an additional contribution to literature studies, opening the way to onsite tests for real-life applications.

The tested beam was loaded under displacement control at two points according to a monotonically increasing curve. Results show a proper classification of the occurring cracks, suggesting the used experimental setup as a possible protocol for practical AE measurements, and yet highlight criticalities on the choice of some parameters during the data interpretation and analysis, denoting the necessity for a consensus on experimental aspects to reach the final goal of a standardized technique.

II. Materials and Methods

The whole setup for the experimental procedure described in this paper is represented in Figure 1. One (or more) sensor is placed on the surface of a structure to be tested – in this case a concrete beam – which collects the acoustic emission of occurring damages. The signal of such emission is sent to the AE instrument which decrypts and saves it.

Any AE signals due to micro-crack formation propagating through the concrete are detected by special AE sensors adequately bonded to the specimen. The AE parameters recorded during a load test are threshold, number of hits, count, duration time, peak, and rise time.

In Figure 2 a single hit is described, and considering the aforementioned parameters it is possible to define the duration time as the time occurring from the increasing of the amplitude to its returning to zero; the peak as the highest value of amplitude of the signal wave, which is of course related to the severity of the cracking source. Threshold is a specific value of amplitude, chosen to remove the background level of the acoustic emission collected. All the signals with amplitude lower than the threshold are neglected by the collecting system. By fixing the threshold value of amplitude, then, it is possible to define the other parameters: count is the number of times the wave amplitude exceeds the threshold level (for each hit), while rise time is the time occurring between the first time the signal exceeds the threshold level and the time it reaches the peak.

According to these parameters, every hit signal can be associated with a specific crack type. More specifically, to define the crack type corresponding to a specific AE, a parametric analysis is performed, and, as a result, it can lead to the distinction of two possible crack modes: tensile cracks and shear cracks, as shown in Figure 3.

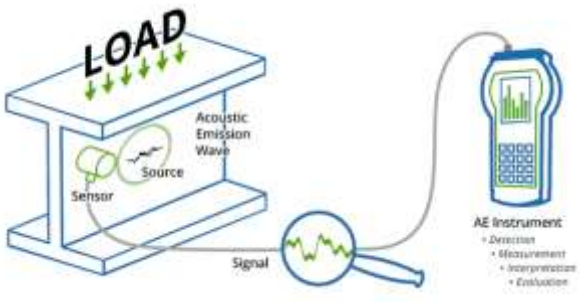

Figure 1. graphical representation of the AE experimental setup, [15].

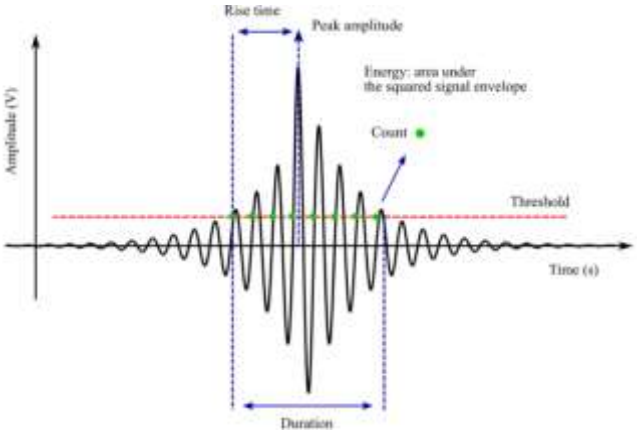

Figure 2. Acoustic parameters recorded in a single hit, [16].

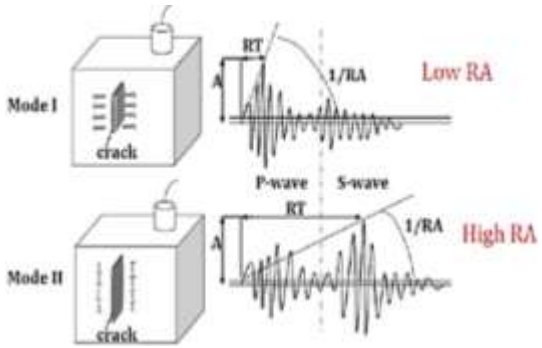

Figure 3. Tensile and shear cracks, [17].

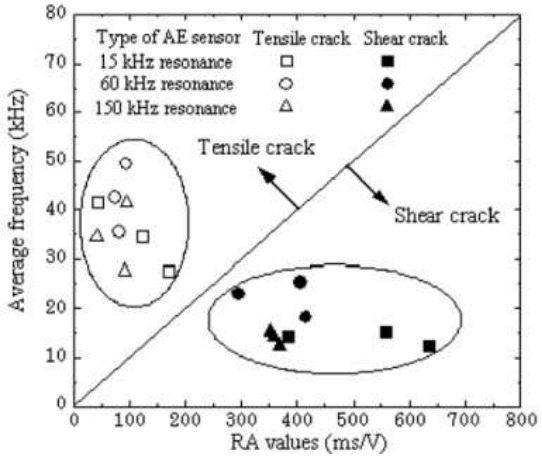

Figure 4. AF and RA correlation. According to RA and AF values, AE hits can be found in a specific region of the graph, specifically above (tensile cracks) or below (shear cracks) the line, [18].

This distinction of the crack type can be performed using two further parameters: Rise Angle (RA) and Average Frequency (AF), which are calculated as in Equation (1) and (2) respectively:

$$RA = \frac{rise\ time}{maximum\ amplitude}\ \left[\frac{ms}{V}\right] \quad (1)$$

$$AF = \frac{counts}{duration\ time}\ [kHz] \quad (2)$$

RA, expressed in *ms/V*, is calculated as the ratio between the rise time and the signal's peak amplitude. Acoustic waves with a high value of RA are characterized by the exploitation of the maximum amplitude of the signal for a long time. At the same time, low RA values are associated with highly energetic acoustic waves occurring in short intervals. AF is defined as the ratio between counts and duration time, meaning that acoustic waves repeatedly exceeding threshold levels over time are characterized by high AF values. Please note that both parameters are affected by the threshold level itself. The final classification of active cracks with RA and AF is performed in Figure 4, [18].

Cracks with low RA and medium-high AF are classified as tensile cracks, whereas events having low AF and medium-high AF are classified as shear cracks. By plotting the bisector, it is easy to notice how much tensile and shear cracks are located respectively above and below the bisector. The specific classification of the cracks' type of plot in Figure 4, of course, strongly depends on the proportion between the axes. In [18], there's a 1:10 proportion, also reported in the JCMS-III B5706 code, [19]. It must be noted that a defined criterion of the proportion between RA and AF does not exist. In the presented application, the chosen RA/AF proportion is 1:1.

III. Case Study Presentation/Experimental Layout

The four-point bending test presented in this work was performed on an RC beam at the StrEngTH laboratory of the Department of Civil Engineering, University of Salerno. The tested concrete was a class C25/30, it had a cross-section measuring 150×200 mm² and a length of 2000 mm, and it was subjected to simple constraints and loaded using displacement control at two points located 625mm away from the supports. During the compression test, it revealed a true cubic compressive strength of 39.33 MPa. The bar was of steel grade B450C, the tensile strength was measured by tensile testing and the yield strength was 551 MPa. As for the acoustic setup, the specimen has been equipped with displacement transducers and three piezoelectric Vallen VS150-RIC sensors to detect and record AE signals. These sensors, depicted in Figure 5 along with their frequency-dependent sensitivity curve, serve as the initial stage of signal detection and preamplification of the crack acoustic signals. They communicate with the ASIP-2 cards, housed in the AMSY-6 chassis, which act as the readout electronics. These signal processors operate at a 40 MHz sampling rate with an 18-bit dynamic range, ensuring high-quality signal acquisition with minimal noise and an excellent signal-to-background noise ratio.

Where the sensors were positioned, a reference axis was established with its origin at the centre of gravity of the beam face This x-axis coincides with the longitudinal axis of the beam (see Figure 6). After measuring the attenuation profile of the AE signal, it was determined that the maximum distance between the sensors was 71.2 cm. Consequently, the spacing between the three sensors was fixed at 50 cm, as illustrated in Figure 6. The sensors were installed on the concrete surface by means of a mechanical vise. The acoustic coupling was granted through the adoption of vaseline or eco-ultrasound gel. This was a crucial point of the experimental setup since the methodology by which the sensors are located can strongly affect the results of the AE detection.

Considering the static scheme and loading conditions (Figure 6), the area of the beam located between the two applied forces is the one experiencing the maximum bending moment. Under these conditions, the upper part of the beam will be in compression.

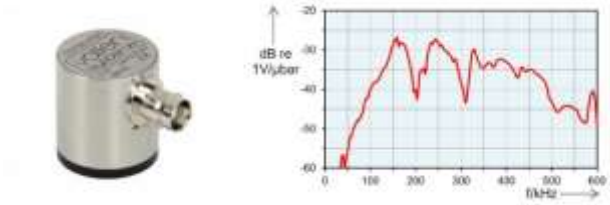

Figure 5. AE sensor picture and its sensitivity curve.

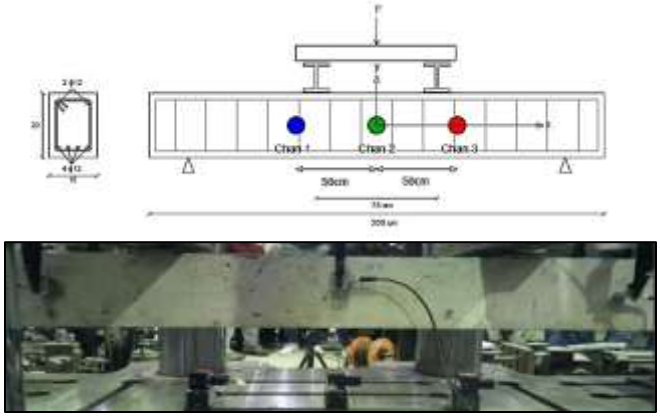

Figure 6. Details of the tested specimen and experimental layout.

This effect increases as the applied load increases and reaches the limit of the concrete cover's capacity. On the other hand, the maximum tension is reached at the bottom of the beam. On the other hand, the regions between the applied force and the supports experience pure shear forces: the bending moment in these regions is linear, with a maximum value at the point of load application and a null point at the support.

Due to this characteristic, the choice of the positioning of the sensor has been strategic since they have been located in the regions where the experienced forces exploit their maximum modulus, and they are the regions where the cracks will happen. Please note that the three sensors are equal, and the differences in detecting the AE signals are only due to their position (see later).

The loading curve is reported in Figure 7 together with the cumulative functions of the hits recorded by each channel. The selected loading protocol is a monotonic increasing curve, as reported in [20], in which a preliminary analysis of the test results performed on the same specimen has been presented. In particular, concerning the tested beam

herein described, in [20], an analysis that involves the localization of AE (Acoustic Emission) events, by combining signals arrivals in each channel, has been performed. Damage localization is one of the main objectives of the Acoustic Emission technique. The read-out and analysis software enables the implementation of a localization processor that correlates signal detection with the location of each sensor, thus identifying the AE source's position. To perform this analysis, it is possible to use the time-of-arrival (TOA) method based on comparing wave arrival times at the various sensors arranged on the structure under test. The time of arrival is detected as the instant at which the signal exceeds the threshold level. Once the hit has been detected by more than one sensor, the TOAs can be used to find the AE source's position and define an event.

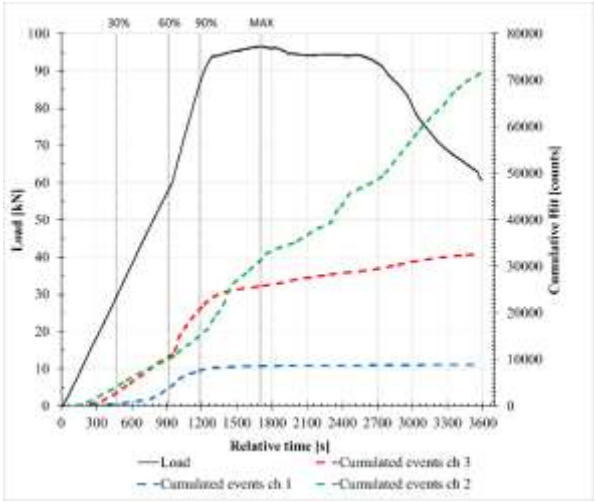

Figure 7. loading curve and hits cumulative functions versus time, [20]

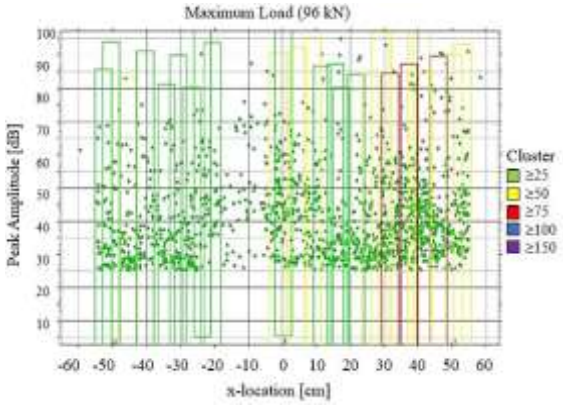

Figure 8. Peak amplitude versus events locations at maximum load, [20]

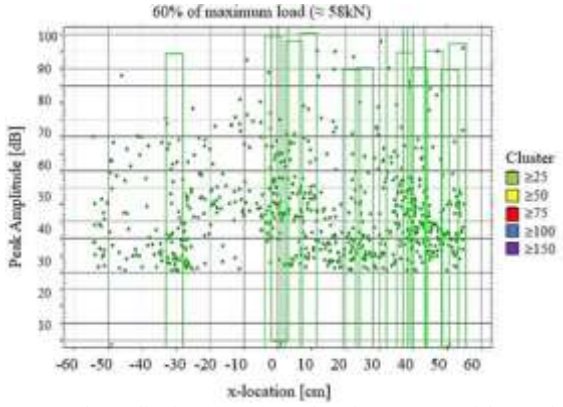

Figure 9. Peak amplitude versus events locations at 60% of the maximum load, [20]

In this way, spatial clusters of events can be drawn to highlight areas of the specimen where a significant activity occurs during the loading test.

The peak amplitude of the localized events can be plotted as a function of the source position. Figure 8 illustrates the localization of AE events at the maximum load. The colored rectangular boxes on the plots correspond to clusters of events, as indicated in the legend on the right side. Notably, the denser clusters of AE events are observed in the center-right part of the beam, confirming the asymmetry of the damage, as will be shown in the next section. Furthermore, in [20], has been underlined that this clustering pattern begins at approximately 60% (Figure 9) of the maximum load, suggesting that this technique can be utilized to predict the failure location. Moreover, acquiring information about the region of the specimen with the highest number of events as the load increases can be valuable in real-life operating conditions, indicating which part of the structure requires further investigation using other diagnostic techniques.

IV. Results and Discussion

After extracting emission data using software, the data were filtered and differentiated based on the acquisition channel. RA and AF parameters were calculated for each detected event to classify the occurring cracks. Subsequently, characterization graphs were prepared to illustrate the progressive stages of loading (30%, 60%, and 90% of the maximum load) for the tested beam.

As a first remark, the analysis of such data has been carried on only on the events having a high number of counts, avoiding collecting signals probably imputing to background noise. As stated before, such filtering strongly depends on the chosen threshold level. The threshold level is set to avoid the collection of background noise. Consequently, the proper analysis of such background level is fundamental for the good results of the experimental procedure. Secondly, for a proper interpretation of the obtained results, it is important to emphasize that the events recorded by each channel are those detected within its vicinity, with a "radius of influence" defined based on the attenuation profile. In particular, as described in section III, in the case study description, the maximum distance within which the sensors detect events is found to be 71.2 cm. However, the sensors are placed at a distance of 50 cm from each other. This configuration implies that there are overlapping detecting zones between the sensors where multiple sensors record events.

Figure 10 represents the AF *vs* RA correlation for all the channels at 30% of the maximum load. The recorded events are located in a region across the bisector, meaning they can be attributed to both tensile and shear solicitations. The maximum AF detected was around 1200 kHz, and the minimum was 200 kHz. RA values span from a minimum of 150 ms/V to a maximum of 1200 ms/V. The graph in Figure 10 reveals important aspects of the generation of cracks and the detection of their acoustic emission. Although the expected response should be symmetrical, in fact, (given the symmetric mechanical properties of the beam and the symmetric application of loads), the response obtained from the AE analysis seems to deviate from symmetry. First of all, several cracks detected by channel 1 have values of AF significantly higher than the values of AF of the events detected by channels 2 and 3 (the number of such events is

even bigger in Figure 11 and Figure 12, where events collected at 60% and 90% of the maximum load are shown). Again, since the cracks are also localized, it can be noticed how the sensor closer to the damaged region is the sensor detecting the highest frequency of the cracks.

As the applied load increases, there is a proportional increase in the number of AEs detected by all sensors, indicating an increasing level of activity and potential damage accumulation. Moreover, the number of events collected at 60% (Figure 11) and 90% (Figure 12) of the maximum load remain on the same region of the plot, meaning that the type of stress generating the acoustic emission (tensile or shear) does not change. The detected acoustic emissions are classified as both tensile and shear.

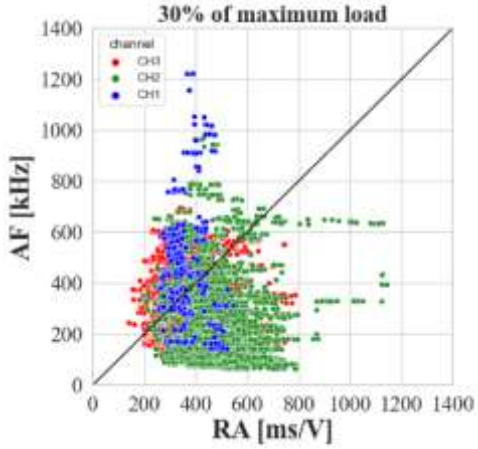

Figure 10. AF vs RA relationship for all the channels at 30% F_{max}. Blu points are related to channel 1, green points are related to channel 2, and red points are related to channel 3.

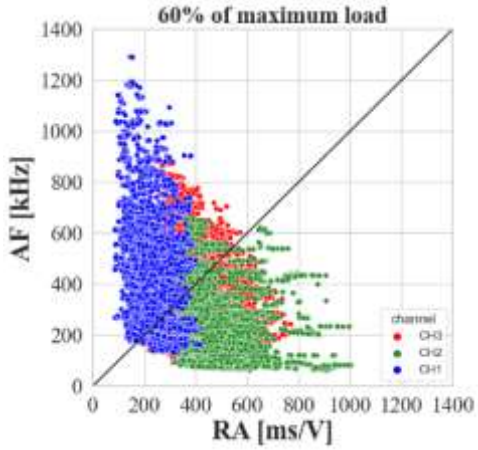

Figure 11. AF vs RA relationship for all the channels at 60% F_{max}. Blu points are related to channel 1, green points are related to channel 2, and red points are related to channel 3.

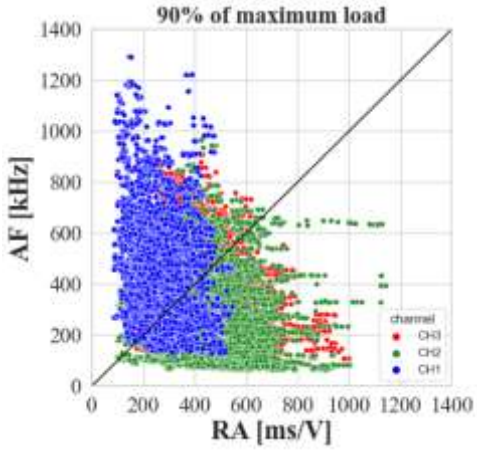

Figure 12. AF vs RA relationship for all the channels at 90% F_{max}. Blu points are related to channel 1, green points are related to channel 2, and red points are related to channel 3.

However, it is noteworthy that a significant increment in AE occurrences is mainly observed in channel 1, passing from 30% to 60% of the maximum load and over. This is probably due to the already mentioned asymmetric resistance of the beam, which leads to a lower AE activity in the left part of the specimen, during the early stage of the test. In addition, even if sensor 1 is located outside the region subjected to pure bending, it detects AEs resulting from the occurrence of combined actions of shear/bending. The aforementioned asymmetric response of the beam explains the detection of mainly tensile and compressive events, respectively in the lower and upper parts of the beam, by sensor 1.

This trend is also observed when applying 90% of the maximum load, as highlighted by the RA/AF correlation determined for each channel and shown in Figure 12. In this last graph, the tendency of channel 1 to mainly detect events related to tensile cracks is confirmed.

The asymmetric behavior observed by the AE analysis is further confirmed by the photographic recording of the beam's surface, as depicted in Figure 13. In this figure, tensile cracks are highlighted in red, while shear cracks are visible on the right side and marked in blue. This visual representation aligns with the AE findings, providing a comprehensive understanding of the different damage mechanisms occurring within the material. Figure 14 shows the beam after the application of the maximum load, confirming once more the asymmetric failure of the specimen.

The obtained results demonstrate the fine capability of the used technique to classify the damages occurring in the tested beam, proving that it configures as a fast and noninvasive method for the early detection, localization, and classification of cracks.

V. Conclusions

In this paper, an AE application on data collected during a four-point bending test on a concrete beam is presented. The AE collection and analysis technique here described can be particularly useful for structural diagnostics, suggesting the possibility of achieving the ambitious goal of correlating measured acoustic emissions with the state of the structure to prevent its damage.

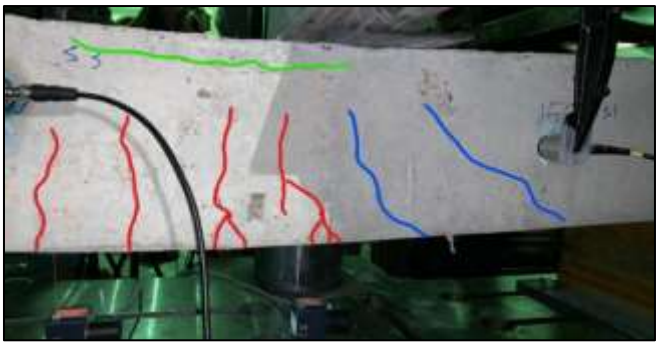

Figure 13. Analysed beam during the test, where cracks are visible. Tensile cracks have been highlighted in red, shear cracks in blue, and compressive cracks in green.

Figure 14. Beam in its ultimate configuration.

In addition, the analysis of AE parameters can lead to an early assessment of the condition of a structure, configuring itself to detect the formation of injuries significantly in advance, and at the same time provide information on their type, well before the maximum load is reached and in any case before the structure irreversibly reaches collapse.

Several parameters of the AE signal have been investigated during the experiment presented in this contribution, the more relevant are threshold, RA, and AF since they determine the following crack classification. Results of the here reported test suggested an unexpected asymmetry in the collection of AE data since the geometry of the experimental setup was organized to preserve the symmetry of the forces applied on the beam. Acoustic events, on the contrary, have been seen to differentiate in type (tensile vs shear) and number between the three different used sensors. This result is probably due to construction dissymmetry, maybe an insufficient transverse reinforcement in the area between sensors 2 and 3 where the rupture occurs. This situation, anyway, did not affect the characterization of the lesions, which turn out to be well-defined by the acoustic emission technique. Finally, the analysis of collected data aroused different remarks on the proper way of choosing the parameters and plotting the data themselves. A proper selection of the threshold value implies a proper count number, which is the parameter determining how many events are identified as proper AE signals. The threshold level is generally depending on the material and the experimental layout, and yet there's no explicit consensus on literature. Threshold level, on its hand, strongly influences RA and AF calculation, and through the calculation of RA (Rise Angle) and AF (Average Frequency) cracks are classified. As a last remark, it is important to underline that the ratio between these two parameters is essential for the crack's classification since it greatly affects the positioning of the events in the graph. Such uncertainty is surely a limitation of the presented work, and yet underlines the necessity to find a consensus on the proper settings of parameters, to achieve a reproducible classification of the cracks' occurring during concrete bending tests.

ACKNOWLEDGMENT

The authors acknowledge the support of "Consorzio della Rete dei Laboratori Universitari di Ingegneria Sismica e Strutturale" (ReLUIS) for funding the research under the project "ReLUIS-Ponti", Sub-task 3.2.1. The authors are grateful to Mariangela Nigro for participating in the data analysis during her bachelor's thesis work.

REFERENCES

[1] S.W. Tang, Y. Yao, C. Andrade, and Z.J. Li, Recent durability studies on concrete structure. Cem Concr Res, 78, 143-154, 2015.

[2] C.B. Scruby, An introduction to acoustic emission, J. Sci. Instrum. 20.8: 946, 1987.

[3] R. Prakash, Non Destructive Testing Techniques. New Academic Science, 2009.

[4] K. Ohno and M. Ohtsu Crack classification in concrete based on acoustic emission, Constr Build Mater, 24(12), 2339-2346, 2010.

[5] C.U. Grosse and F. Florian, Quantitative evaluation of fracture processes in concrete using signal-based acoustic emission techniques, Cem Concr Compos Composites 28.4: 330-336, 2006.

[6] K. Ohno, K. Uji, A. Ueno and M. Ohtsu,. Fracture process zone in notched concrete beam under three-point bending by acoustic emission. Constr Build Mater 67,139–145, 2014.

[7] M.A.A Aldahdooh, N.M. Bunnori and M.M. Johari, Damage evaluation of reinforced concrete beams with varying thickness using the acoustic emission technique, Constr Build Mater 44,812–821, 2013.

[8] N.M Nor, N.M. Bunnori, A. Ibrahim, S.Shahidan and S.N.M. Saliah, "Relationship between acoustic emission signal strength and damage evaluation of reinforced concrete structure: Case studies", in IEEE Symposium on Industrial Electronics and Applications ISIEA2011, September 25-28, 2011, Langkawi, Malaysia.)

[9] L. Golaski, G. Pawel and O. Kanji, Diagnostics of reinforced concrete bridges by acoustic emission, J. Acoust. Emiss. 20.1 83-98, 2002

[10] A. Nair and C.S. Cai, Acoustic emission monitoring of bridges: Review and case studies, Eng. Struct, 32.6 1704-1714, 2010

[11] M.J. Šofer, Cienciala, M. Fusek, P. Pavlíček, and R. Moravec, Damage analysis of composite CFRP tubes using acoustic emission monitoring and pattern recognition approach, Materials 14.4 786, 2021

[12] A. Sánchez Roca, H. Carvajal Fals, J. Blanco Fernández, F. Sanz Adán and E. Jiménez Macías, Stability analysis of the gas metal arc welding process based on acoustic emission technique, Weld Int 23.3: 173-180, 2009.

[13] N.A. Lamberti, M. La Mura, C. Guarnaccia, G. Rizzano, J. Quartieri and N.E. Mastorakis, "An ultrasound technique for the characterisation of the acoustic emission of reinforced concrete beam" in Applied physics, system science and computers II. Cham (Ntalianis K and Croitoru A (eds) Springer International Publishing, 2019), pp. 63–68.

[14] C. Chisari, C. Guarnaccia, N. Lamberti, V. Piluso, J. Quartieri and G. Rizzano, Acoustic Emissions analysis of a four-point bending test on a Reinforced Concrete beam, Struct. Health Monit. 19(2), 2017.

[15] Overview of Acoustic Emission NDT Technology, Physical Acoustics AE Technology. Available online: https://www.physicalacoustics.com/ae-technology/ (last accessed on July 27, 2023).

[16] M. Nani Babu, C.K. Mukhopadhyay and G. Sasikala. Fatigue crack growth study in p91 and 316LN steels using acoustic emission, Trans. Indian Inst. Met., 72: 3067-3080, 2019.

[17] G. Lacidogna, G. Piana and A. Carpinteri, Acoustic emission and modal frequency variation in concrete specimens under four-point bending, Appl Sci 7.4: 339, 2017.

[18] M. Ohtsu, T. Isoda and Y. Tomoda, Acoustic emission techniques standardised for concrete structures, J. Acoust. Emiss. 25: 21-32, 2007.

[19] JCMS-III B5706, Monitoring Method for Active Cracks in Concrete by Acoustic Emission, Federation of Construction Materials Industries, Japan, 2003.

[20] P. Barra, A.B. Francavilla, D. Rossi, M. Latour, C. Guarnaccia and G. Rizzano, Acoustic Emissions Detection and Analysis during a 4 Points Bending Test on a Reinforced Concrete Beam, presented at the Int. Conf. on Applied Physics, Simulation and Computing (APSAC 2023), Journal of Physics: Conference Series, 2023, *in press.*

Contribution of individual authors to the creation of a scientific article (ghostwriting policy)

Conceptualization: C. Guarnaccia, G. Rizzano, M. Latour
Data curation: A.B. Francavilla, P. Barra, D. Rossi, C. Guarnaccia
Funding Acquisition: G. Rizzano, M. Latour
Investigation: A.B. Francavilla, C. Guarnaccia, G. Rizzano
Methodology: A.B. Francavilla, C. Guarnaccia, G. Rizzano
Software: A.B. Francavilla D. Rossi, P. Barra, C. Guarnaccia
Supervision: C. Guarnaccia, G. Rizzano, M. Latour
Writing - original draft: P. Barra, A.B. Francavilla D. Rossi
Writing - review & editing: all the co-authors

Sources of funding for research presented in a scientific article or scientific article itself

The research was partially funded by "Consorzio della Rete dei Laboratori Universitari di Ingegneria Sismica e Strutturale" (ReLUIS) under the project "ReLUIS-Ponti", Sub-task 3.2.1.

Conflict of Interest

The authors have no conflict of interest to declare that is relevant to the content of this article.